Cell

A CK2-Dependent Mechanism for Degradation of the PML Tumor Suppressor

Pier Paolo Scaglioni,[1,2] Thomas M. Yung,[1,3] Lu Fan Cai,[1,3] Hediye Erdjument-Bromage,[4] Andrew J. Kaufman,[5] Bhuvanesh Singh,[5] Julie Teruya-Feldstein,[3] Paul Tempst,[4] and Pier Paolo Pandolfi[1,3,*]
[1] Cancer Biology and Genetics Program, Sloan-Kettering Institute
[2] Department of Medicine
[3] Department of Pathology
[4] Molecular Biology Program, Sloan-Kettering Institute
[5] Department of Surgery
Memorial Sloan-Kettering Cancer Center, New York, NY 10021, USA
*Contact: p-pandolfi@ski.mskcc.org
DOI 10.1016/j.cell.2006.05.041

SUMMARY

The PML tumor suppressor controls key pathways for growth suppression, induction of apoptosis, and cellular senescence. PML loss occurs frequently in human tumors through unknown posttranslational mechanisms. Casein kinase 2 (CK2) is oncogenic and frequently upregulated in human tumors. Here we show that CK2 regulates PML protein levels by promoting its ubiquitin-mediated degradation dependent on direct phosphorylation at Ser517. Consequently, PML mutants that are resistant to CK2 phosphorylation display increased tumor-suppressive functions. In a faithful mouse model of lung cancer, we demonstrate that *Pml* inactivation leads to increased tumorigenesis. Furthermore, CK2 pharmacological inhibition enhances the PML tumor-suppressive property in vivo. Importantly, we found an inverse correlation between CK2 kinase activity and PML protein levels in human lung cancer-derived cell lines and primary specimens. These data identify a key posttranslational mechanism that controls PML protein levels and provide therapeutic means toward PML restoration through CK2 inhibition.

INTRODUCTION

Aberrant ubiquitin-proteasome-dependent degradation of tumor-suppressor proteins is a key oncogenic force underlying human tumorigenesis. Importantly, substrate recognition is often mediated by phosphorylation events (Pagano and Benmaamar, 2003). The $p19^{ARF}$-Mdm2-p53 and Skp2-$p27^{Kip1}$ pathways are perhaps the most well-established examples where overactivation of the ubiquitin-proteasome machinery plays a key role in the pathogenesis of common human cancers (Michael and Oren, 2002; Pagano and Benmaamar, 2003).

The promyelocytic leukemia gene (*PML*) is a tumor suppressor that was originally identified as a component of the PML-RARα oncoprotein of acute promyelocytic leukemia (APL) (Piazza et al., 2001; Salomoni and Pandolfi, 2002 and references therein). PML localizes to nuclear-matrix-associated macromolecular structures known as PML nuclear bodies (NBs), which are dependent on PML for assembly (Zhong et al., 2000). PML phosphorylation is known to mediate its proapoptotic activity (Bernardi et al., 2004; Hayakawa and Privalsky, 2004; Yang et al., 2002).

PML plays a critical role in growth control, transformation suppression, induction of apoptosis, and replicative senescence depending on the cellular context. *Pml* inactivation in mice results in cancer susceptibility (Salomoni and Pandolfi, 2002; Trotman et al., 2006; Wang et al., 1998). In addition, it has been reported that PML protein is completely or partially lost in a large fraction of human cancers and that loss of PML protein correlates with tumor progression. In these cases, sequence analysis of the *PML* gene and promoter methylation studies revealed no inactivating mutations or aberrant methylation while mRNA transcripts were consistently detected, suggesting that PML is aberrantly degraded in human cancer (Gurrieri et al., 2004; Koken et al., 1995).

Treatment with arsenic trioxide and viral infection also results in degradation of PML protein and disruption of the PML NBs (Everett, 2001; Lallemand-Breitenbach et al., 2001). However, it is currently unknown which mechanisms regulate PML protein levels under these conditions.

Here we describe the identification of a PML kinase whose activity depends on the α subunit of casein kinase

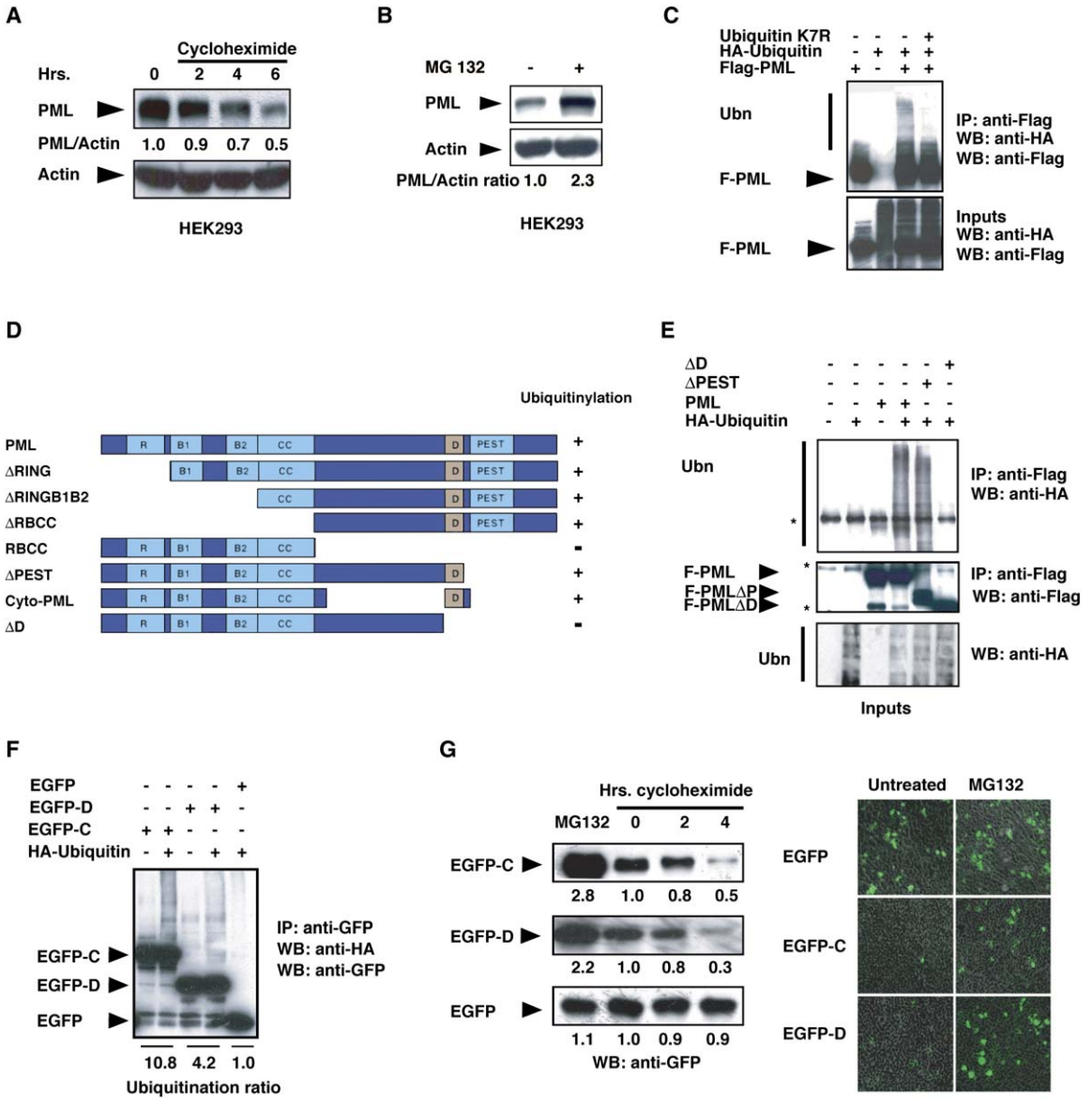

Figure 1. PML Is Polyubiquitylated and Degraded in a Proteasome-Dependent Manner

(A) PML undergoes degradation in HEK293 cells. Endogenous PML and actin proteins were detected by Western blot (WB) in cycloheximide-treated cells.

(B) Proteasome inhibition leads to PML upregulation. HEK293 cells were treated with MG132 as indicated. Endogenous PML and actin were detected by WB.

(C) PML is polyubiquitylated. HEK293 cells were transfected and analyzed by immunoprecipitation (IP) and WB as indicated (upper panel). Note that the membrane was not stripped in between hybridizations. Ten percent of the input lysate was analyzed by WB (lower panel). Ubn = polyubiquitin chains.

(D) Schematic representation of informative constructs used in this study. PML modular organization is represented along with its major domains. Boxes in light blue and light brown represent PML domains. R: RING finger; B1 and B2: B boxes: CC: coiled coil; D: degron; PEST: PEST domain. The column on the right indicates whether mutant PML proteins undergo polyubiquitylation.

(E) Deletion of a critical PML C-terminal protein sequence abrogates PML ubiquitylation. HEK293 cells were transfected as indicated, and their lysates were analyzed by IP and WB. Ten percent of the input lysate was analyzed by WB with an anti-HA antibody (lower panel). * = background bands.

(F) A critical PML C-terminal protein sequence is sufficient to cause ubiquitylation of EGFP. HEK293 cells were transiently transfected with a vector expressing EGFP-C, EGFP-D, or wild-type EGFP. HA-ubiquitin was cotransfected as indicated and analyzed by IP and WB. Note that the membrane was not stripped in between hybridizations. Intensity of the polyubiquitin chains is expressed as a ratio between polyubiquitylated EGFP proteins and EGFP protein input.

(G) A critical PML C-terminal sequence is sufficient to cause proteasome-mediated degradation of EGFP. HEK293 cells were transiently transfected and treated as indicated and were analyzed by WB. Representative fields of EGFP-positive cells obtained from the same transfection are presented in the right panels. Note that MG132 upregulates EGFP-C and EGFP-D, but not EGFP.

2 (CK2). CK2 is a nuclear-matrix-associated, highly conserved, and ubiquitous serine/threonine kinase that consists of two catalytic ($\alpha\alpha$, $\alpha'\alpha'$ or $\alpha\alpha'$) and two β regulatory subunits (Pinna, 2002). The regulation and function of CK2 are not well defined, and, traditionally, CK2 has been considered a constitutively nonregulated protein kinase (Allende and Allende, 1995). However, it has been shown recently that CK2 is a stress-activated protein kinase implicated in prosurvival functions through the phosphorylation of substrates such as IκBα. (Ahmed et al., 2002; Kato et al., 2003; Litchfield, 2003). Importantly, CK2 is frequently activated in human cancers and can induce mammary tumors and lymphomas when expressed in transgenic mice (Landesman-Bollag et al., 2001; Seldin and Leder, 1995). Consistent with these findings, we report that CK2-mediated PML phosphorylation plays a critical role in causing PML polyubiquitylation and degradation upon cellular stress and carcinogenesis.

RESULTS

PML Undergoes Ubiquitin-Proteasome-Mediated Degradation

We determined whether PML is degraded in immortalized and tumor-derived cell lines. PML has a half-life of about 3 hr in HEK293, NIH 3T3, and Colo320DM cell lines but a half-life greater than 6 hr in primary mouse embryonic fibroblasts (MEFs) (Figure 1A; see also Figures S1A–S1C in the Supplemental Data available with this article online). Treatment of HEK293 cells with proteasome inhibitors such as MG132 or lactacystin (data not shown) led to increased PML levels (Figure 1B). We concluded that PML undergoes degradation in immortalized and tumor-derived cell lines.

To test whether PML undergoes ubiquitylation, we expressed Flag-tagged PML in HEK293 cells together with HA-ubiquitin and treated them with MG132. Immunoprecipitation (IP) followed by Western blot (WB) analysis detected a ladder of HA-marked PML polypeptides. Cotransfection with a vector expressing ubiquitin K7R, a mutant that has all seven lysine residues substituted by arginine and hence is unable to form polyubiquitin chains, abrogated the ladder of HA-marked PML polypeptides (Figure 1C). We obtained similar results using express-tagged PML, providing further evidence that PML itself and not other coimmunoprecipitating proteins underwent ubiquitylation (data not shown). We concluded that regulation of PML turnover involves an ubiquitin-dependent proteasome pathway.

Identification of the PML Degron

PML is a phosphoprotein that contains N-terminal and C-terminal predicted PEST domains. These sequences are associated with proteins that are rapidly degraded upon phosphorylation. To map the protein sequence necessary and sufficient to direct PML ubiquitylation, we generated a large series of PML deletion mutants that we screened upon transfection with HA-ubiquitin in HEK293 cells for the ability to be conjugated to polyubiquitin chains. A representative example of our analysis is presented in Figure 1E. The results, summarized in Figure 1D, indicate that the PML degron lies between amino acids 498 and 524.

We next tested whether the PML 498–524 sequence is sufficient to direct polyubiquitylation of a heterologous protein. We found that EGFP-C and EGFP-D were readily conjugated to polyubiquitin chains in HEK293 cells, while EGFP was not (Figure 1F). We also found that EGFP proteins containing the PML 498–524 protein sequence have a half-life of about 3 hr in HEK293 cells and that their levels are upregulated by proteasome inhibition (Figure 1G). These results indicate that the PML 498–524 protein sequence is necessary and sufficient to direct ubiquitin-proteasome-mediated protein degradation. Accordingly, we defined this sequence as the PML degron.

CK2 Phosphorylates the PML Degron Directly

Protein sequence analysis of the PML degron with the Scansite (http://scansite.mit.edu) and ELM (Eukaryotic Linear Motif, http://elm.eu.org) prediction algorithms revealed the presence of multiple phosphorylation consensus sites for CK2 (Figure 2A). Of note, S512 is a low-probability CK2 consensus site in unmodified PML that becomes a high-probability CK2 consensus site when S517 is phosphorylated (Meggio et al., 1984; Meggio and Pinna, 2003). Thus, we tested whether CK2 directly phosphorylates PML in vitro. As shown in Figure 2B, recombinant CK2 readily phosphorylates bacterially expressed PML in an immunocomplex kinase assay.

We found that concomitant abrogation of S512, S513, S514, and S517 reduced PML phosphorylation by CK2 more than 90%, while S517 abrogation alone reduced PML phosphorylation by more than 85%. In contrast, the S512–514A mutations reduced PML phosphorylation by about 40% (Figure 2B). In addition, concomitant abrogation of S512–514, S517, and S529–531 completely abrogated PML phosphorylation by CK2 (data not shown). These data indicate that PML S517 is the primary CK2 phosphorylation site and suggest that phosphorylation of this serine primes phosphorylation of S514. In addition to S514 and S517, minor phosphorylation sites exist in the downstream PML PEST sequence.

Next, we tested whether lysates of tumor cell lines where PML is polyubiquitylated contain a protein kinase activity that phosphorylates PML under native conditions. We readily detected a PML kinase activity that was markedly inhibited by preincubation of the cell lysates with TBB, a specific CK2 inhibitor (Figure 2C). His-PML S517A was barely phosphorylated in this assay.

To confirm that the PML 498–524 protein sequence does indeed contain the phosphoacceptor site for CK2, we analyzed full-length CK2 phosphorylated PML (P-PML) and unphosphorylated PML (C-PML) by MALDI-reTOF mass spectrometry. One m/z peak, at 1947.84 atomic mass units (amu), was observed in the spectra of P-PML and was absent from C-PML. The m/z value

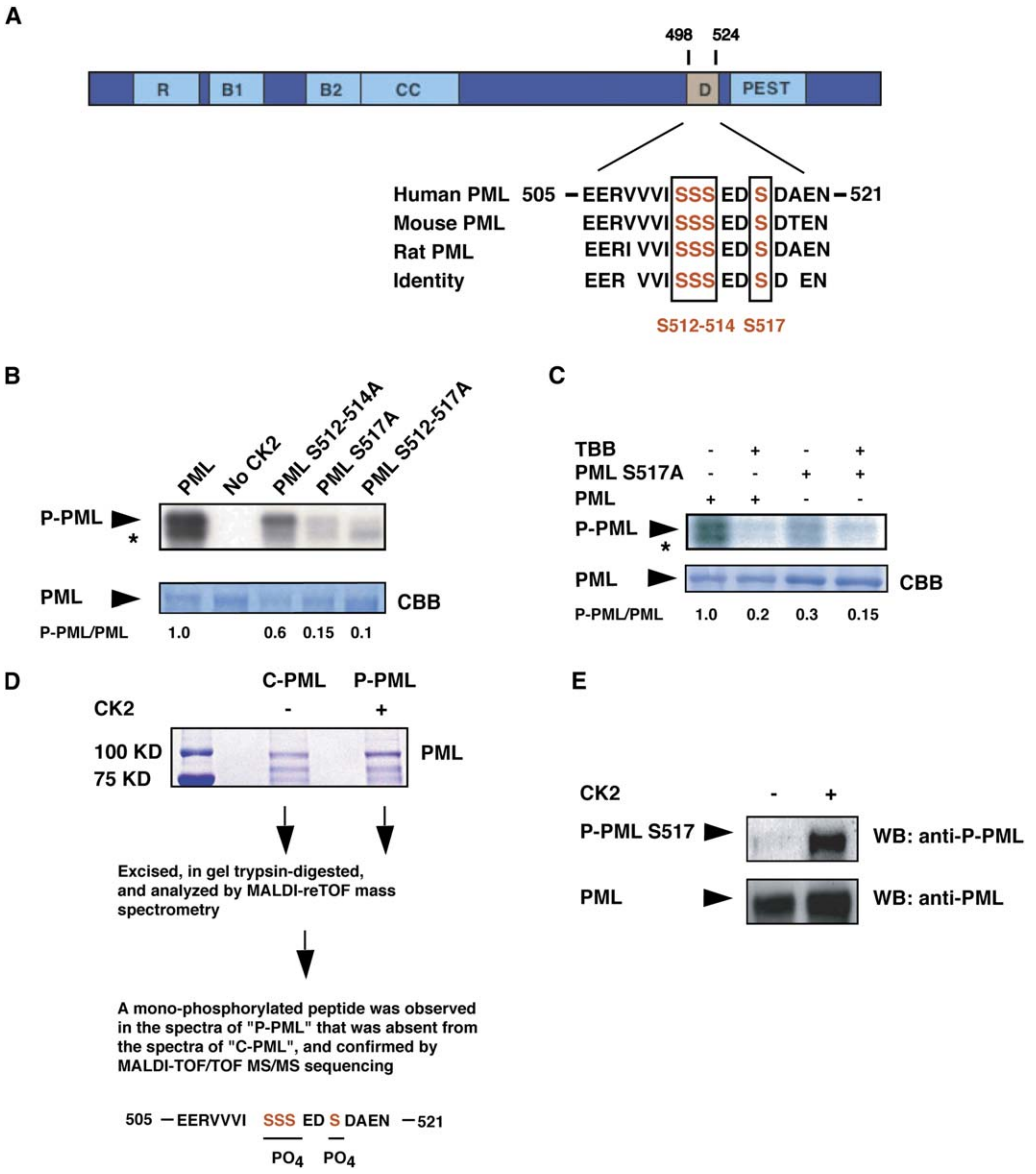

Figure 2. The PML Degron Is Phosphorylated In Vitro by CK2

(A) Schematic representation of PML modular organization along with its major domains. Serines conserved in human, mouse, and rat PML are shown in red. Boxes indicate serines 512–514 and 517.

(B) PML S517 is the primary direct CK2 phosphorylation site in vitro. In vitro kinase assay was performed with bacterially produced His-PML and CK2 proteins. Phosphorylated PML was detected by autoradiography after SDS-PAGE. Protein inputs are shown (lower panel). The intensity of the bands is expressed as a ratio between phosphorylated PML (P-PML) and PML protein. * = background bands; CBB = Coomassie brilliant blue.

(C) Cellular CK2 is required for PML phosphorylation and depends on S517. Bacterially produced His-PML and His-PML S517A were incubated with HEK293 cell lysates, immobilized on nickel beads, incubated with γ-ATP in a kinase assay, resolved by SDS-PAGE, and autoradiographed. TBB was added when indicated.

(D) S512–517 contains the primary direct CK2 phosphorylation site. Bacterially expressed His-PML was incubated with or without recombinant CK2 in an in vitro kinase assay. Phosphorylation-site mapping was determined by mass spectrometry. P-PML: His-PML incubated with CK2. C-PML: His-PML incubated without CK2. The sequence of the peptide containing the phosphorylated serines is underlined.

(E) An antiserum raised against a phosphorylated PML Ser517 (P-PML S517) recognizes PML phosphorylated by CK2. Bacterially expressed His-PML was incubated with and without CK2 in an in vitro kinase assay and analyzed by WB with the anti-P-PML S517 and, after membrane stripping, with the anti-PML antibody (upper and lower panels, respectively).

mapped to a predicted, monophosphorylated fragment of the PML sequence (VVVISSSEDSDEANSSSR) with a mass discrepancy of less than 17 ppm (0.034 Da) for the monoisotopic peak. This precursor ion was then selected for MALDI-TOF/TOF MS/MS analysis. Presence of unique fragment ions confirmed the identity and the

monophosphorylation state (characteristic, partial loss of 98 amu) of this peptide and further allowed us to narrow the site of phosphorylation down to S512, S513, S514, or S517 in the PML sequence (VVVISSSEDSDEANSSSR). In view of the sequence specificity of CK2 and the results obtained in the in vitro kinase assays, we concluded that S517 was the residue directly phosphorylated by CK2 (Figure 2D). However, while S517 is the predominant site of CK2-mediated phosphorylation, we obtained some fragmentary experimental data indicating that additional phosphorylation sites may exist (data not shown). Their phosphorylation status may vary depending on the experimental conditions or may not be identified because of the sensitivity limit of the analysis. Furthermore, we found that recombinant PML phosphorylated in vitro by CK2 is efficiently recognized in WB by an antiserum raised against a peptide containing phosphorylated PML S517 (anti-P-PML S517) (Figure 2E). These experiments suggest that PML is efficiently phosphorylated by CK2 at physiological concentrations under native conditions and prove that PML S517 is the major CK2 acceptor site.

p38 MAPK Activation Is Required for PML Degradation

Since during cellular stress, CK2 activation depends on p38 MAPK, we investigated whether p38 MAPK activation leads to PML polyubiquitylation and degradation (Kato et al., 2003; Sayed et al., 2000). Treatment of NIH 3T3 cells with 0.5 M sorbitol, a well-established and selective p38 MAPK activator, led to a striking reduction of endogenous PML protein that was maximal after 60 min of treatment. As expected, p38 MAPK activation occurred at early time points after treatment (Figure 3A). No obvious loss of cell viability was observed by trypan blue exclusion (data not shown). Furthermore, we found that sorbitol induced a decrease in PML protein accompanied by an increase in PML polyubiquitylated species (Figure 3B). In this case, incubation with MG132 was omitted due to its absolute toxicity in the setting of osmotic shock (data not shown). We also found that treatment with anisomycin and UV radiation, two other well-established p38 MAPK activators, led to marked PML downregulation in NIH 3T3 cells (data not shown). As these treatments may activate other stress-activated kinases, such as the c-Jun N-terminal kinases (JNKs), we utilized *Jnk1/2*$^{-/-}$ immortalized MEFs, in which we noticed similar results (Figures S2A and S2B). Next, we found that inhibition of p38 MAPK with p38AF, a dominant-negative mutant, or the specific inhibitor SB202190 efficiently blocked PML degradation in NIH 3T3 cells (Figures 3C and 3D). Thus, we concluded that sorbitol-induced PML degradation is dependent on p38 MAPK activity.

Finally, we found that PML was markedly phosphorylated upon sorbitol treatment and that its maximal phosphorylation occurred after 1 hr of treatment, at the same time as its maximal downregulation (Figure 3E). These results demonstrate that, upon osmotic shock, PML is phosphorylated by a kinase activity that depends on p38 MAPK.

CK2 Is Required for PML Degradation

We found that the PML protein kinase activity present in the cellular lysates was dramatically stimulated by sorbitol treatment and was sensitive to TBB treatment. In addition, a PML degron mutant carrying alanine-to-serine substitutions that abrogate the CK2 phosphorylation consensus sites was not phosphorylated upon sorbitol treatment (Figure 4A). Next, we found that TBB and K25 (another specific CK2 inhibitor) abrogate osmotic-shock-induced PML degradation (Figure 4B). In addition, PML and CK2 colocalize in the nucleus (Figure S3A). These data collectively indicate that CK2 is the major PML kinase present in HEK293 lysates and that osmotic shock significantly upregulates CK2 kinase activity.

We found that two specific siRNA oligonucleotides caused a 75% reduction in CK2α protein in NIH 3T3 cells. Endogenous PML protein was more than twice the levels observed in cells treated with scrambled siRNA (Figure 4C). We did not find detectable CK2α' protein by WB in the cells used for this study and did not find it necessary to perform RNAi experiments against CK2α' (P.P.S., T.M.Y., and P.P.P., unpublished data). These experiments confirm that CK2 kinase is required for PML degradation.

Furthermore, we found that concomitant abrogation of PML S512–514 and S517 or of the single PML S517 resulted in complete resistance to sorbitol-induced degradation, while abrogation of PML S512, S513, and S514 resulted in partial resistance (Figure 4D). These experiments further validate that PML phosphorylation by CK2 is essential for its osmotic-shock-induced degradation.

In order to further investigate the relevance of S517 in CK2-induced PML degradation, we reconstituted MEFs derived from *Pml*$^{-/-}$ mice with wild-type PML and PML S517A. Pools of retrovirally transduced cells were treated with UV radiation (60 J/m^2). In untreated cells, PML S517A protein was about twice the amount of wild-type PML. This disparity was not due to different expression of wild-type and mutant PML mRNA as assessed by quantitative real-time PCR. Wild-type PML was degraded upon UV treatment, while PML S517A was not (Figure 4E). In addition, we found that PML S517D, a phosphomimetic mutant, displays substantially increased levels of polyubiquitylation in HEK293 cells and formed smaller nuclear body-like structures in *Pml*$^{-/-}$ MEFs (Figure 4F and Figure S3B). Finally, we found that PML maximal phosphorylation within the cell occurred after 30 min of UV treatment (Figure 4G). As expected, PML phosphorylation was abolished by treatment with TBB. These results demonstrate that PML S517 is the major phosphoacceptor site in vivo and that phosphorylation of this site is required for ubiquitylation.

Mutations at S517 Affect PML Stability and Tumor-Suppressive Function In Vitro and In Vivo

We hypothesized that PML null cells reconstituted with PML S517A would be more sensitive to proapoptotic stimuli. Consistent with our previous report, PML sensitized cells to UV-induced apoptosis (Salomoni et al., 2005).

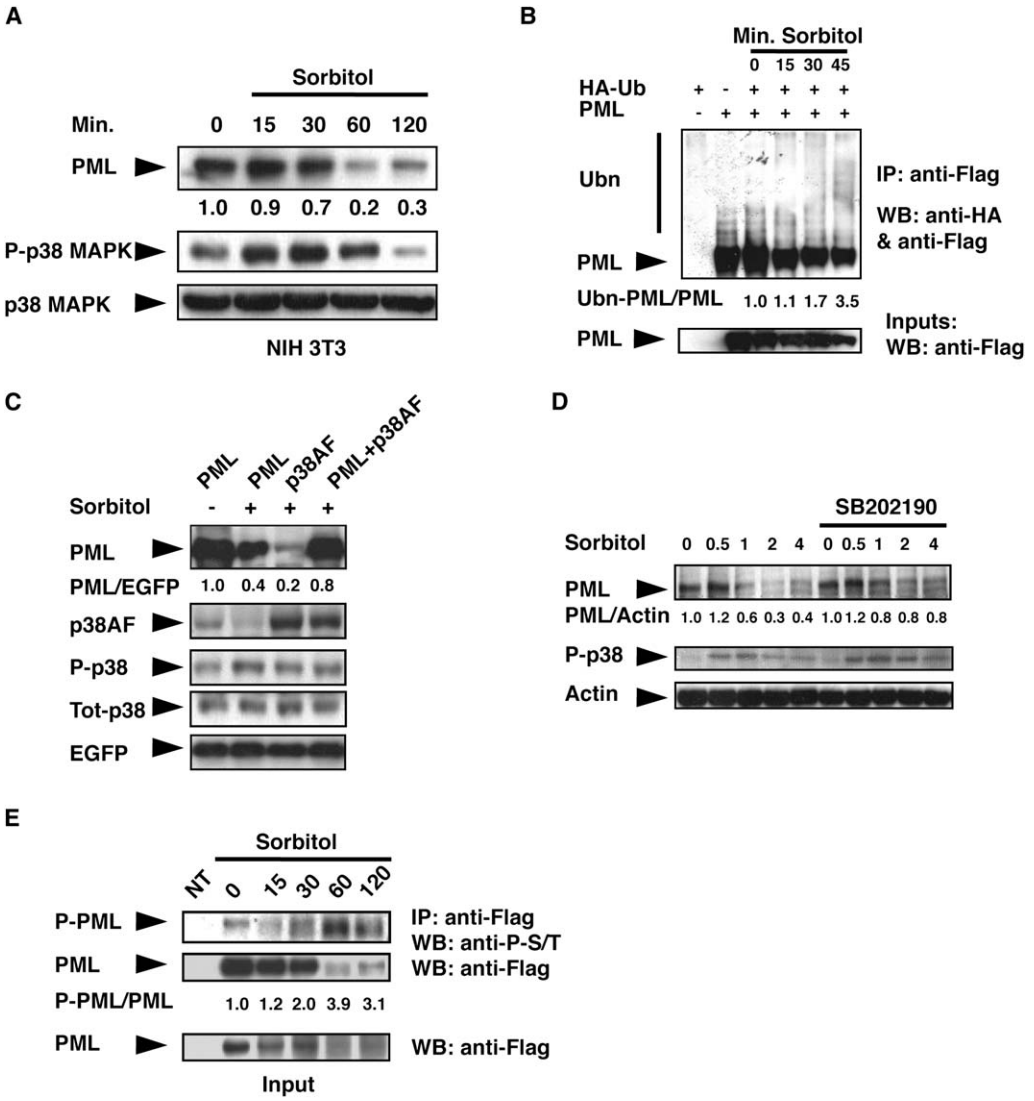

Figure 3. p38 MAPK-Mediated CK2 Activation Is Required for PML Polyubiquitylation

(A) Osmotic shock leads to PML downregulation. NIH 3T3 cells were treated with sorbitol as indicated. Endogenous proteins were detected by WB (upper panel).

(B) Osmotic shock leads to PML polyubiquitylation. HEK293 cells were transfected, treated, and analyzed by IP and WB as indicated. The membrane was not stripped in between hybridizations. Cells were not treated with MG132. Ten percent of the input was analyzed by WB (lower panel). The polyubiquitylated PML/PML ratio is indicated. Ubn = polyubiquitin chains; Ubn-PML = polyubiquitylated PML.

(C) PML downregulation by sorbitol is inhibited by p38AF, a dominant-negative p38 MAPK mutant. HEK293 cells were transfected and, when indicated, treated with sorbitol for 1 hr. Proteins were analyzed by WB.

(D) PML downregulation by sorbitol is inhibited by a specific p38 MAPK inhibitor. NIH 3T3 cells were incubated in the presence of SB202190, treated with sorbitol as indicated, and analyzed by WB.

(E) PML is phosphorylated upon osmotic shock. HEK293 cells were transfected, treated with sorbitol as indicated, and analyzed by IP and WB (upper panels). Ten percent of the IP input was analyzed by WB (lower panel).

PML S517A further increased the percentage of apoptotic cells in agreement with its resistance to UV-induced degradation (Figure 4E and Figure 5A). Thus, UV-induced PML degradation, which depends on its phosphorylation by CK2, protects cells against UV-induced apoptosis.

Next, we tested the biological properties of PML S517A in a senescence assay using WI38 primary human fibroblasts, in which PML overexpression triggers cellular senescence (Bischof et al., 2002). We found that a higher percentage of PML S517A-transduced WI38 cells expressed SA-β-Gal when compared to cells transduced with wild-type PML or empty vector (Figure 5B). Population doublings were also reduced in cells transduced with PML S517A. As expected, PML S517A protein levels

were significantly higher than the wild-type PML protein levels, while there was no difference in their mRNA levels (Figure 5C). These data suggest that PML S517A behaves as a superactive PML mutant due to defective CK2-mediated degradation.

We next examined the tumor-suppressive role of wild-type PML, PML S517A, and PML S517D in vivo. We utilized Colo320DM cells, in which PML is degraded in a CK2-dependent manner (Figure 6D). As expected, PML protein levels in transduced cells were as follows: PML S517A > wild-type PML > PML S517D. Transduced cells were injected subcutaneously into athymic nude mice. When compared with mock-infected cells, expression of wild-type PML or PML S517D did not inhibit tumorigenicity in vivo, while PML S517A-expressing cells showed a >50% reduction in tumor size (Figure 5D).

We next determined whether PML protein levels would dictate the degree of growth/tumor suppression both in vitro and in vivo, in turn suggesting that the enhanced biological effects of PML S517A are due to its increased stability. Utilizing a double retroviral transduction strategy, we generated Colo320DM cells that overexpress wild-type PML at levels greater than PML S517A. Colo320DM cells were cotransduced with empty pBabe Puro and pWzl Hygro retroviral vectors, pBabe Puro and pWzl Hygro PML (^{H}PML), pBabe Puro and pWzl Hygro PML S517A (^{H}PML S517A), or pBabe Puro PML (^{P}PML) and ^{H}PML. Doubly transduced cells were selected by culture in medium containing puromycin and hygromycin. As expected, PML S517A protein level was twice that of wild-type. Cells cotransduced with ^{P}PML and ^{H}PML expressed more than 3-fold more wild-type PML than singularly transduced cells. Growth-curve analysis of pooled cell populations revealed a striking growth inhibition that correlated with the amount of PML protein (Figure S4). Next, we found that in vivo transduction with ^{H}PML and ^{P}PML resulted in inhibition of tumor growth >70%, while transduction with ^{H}PML S517A induced a reduction in tumor size of about 50% as compared to wild-type PML (Figure 5E).

Taken together, these experiments strongly suggest that the inhibition of tumorigenicity is directly dependent on PML protein levels and that phosphorylation of S517 by CK2 abrogates the tumor-suppressive activity of PML, triggering its proteasome-dependent degradation.

CK2-Dependent Degradation of PML in Tumor-Derived Cell Lines and Human NSCLC

PML is often partially or completely lost in non-small cell lung cancer (NSCLC) (Gurrieri et al., 2004; Koken et al., 1995), while CK2 is overexpressed and amplified in NSCLC, where it predicts poor survival (O-charoenrat et al., 2004). Therefore, we tested for an inverse correlation between the two in a panel of NSCLC cell lines and primary human NSCLC specimens. The cell lines could be divided into two groups based on the relative amount of PML protein. In A549, H1299, and H322, PML protein was barely detectable. On the contrary, PML protein was easily detected in H2030, H157, H1975, H1650, and H358 cells (Figure 6A). We performed a CK2 kinase assay on H1299 and H322 cells and H1650 and H358 cells (representative of cells with high and low PML protein levels, respectively). CK2 kinase activity was strikingly elevated in H322 and H1299 as compared to H1650 and H358 cell lines (Figure 6B). TBB upregulated PML protein levels in H322 and H1299 cells (Figure 6C) but had little or no effect on PML in H1650 and H358 cells (Figure S5C). TBB similarly upregulated PML in HEK293 and Colo320DM cells, in which CK2 kinase activity is upregulated as compared to MEFs (Figure 6D and Figure S4D). Transduction of a CK2-resistant PML S517A mutant exerted increased growth-inhibitory effects compared to wild-type PML in NSCLC cells with high CK2 kinase activity (Figure 6E). Since it has been reported that CK2 and PML have opposing effects on the NF-κB pathway (Wu et al., 2003), we assessed NF-κB transcriptional activity in our panel of NSCLC cells. Surprisingly, we found no correlation between NF-κB transcriptional activity and CK2 kinase activity and hence no correlation with PML protein levels. We also found no effect of PML or PML S517A overexpression on NF-κB transcriptional activity in the NSCLC cell lines with high CK2 activity or in Colo320DM cells (Figures S5A and S5B and data not shown). Wild-type and PML S517A proteins were expressed as expected (Figure S5E). These results indicate that, at least in the cell lines utilized in this study, the PML and NF-κB pathways do not appear to crosstalk, while CK2 activity results in a decrease of PML protein.

Pml Inactivation Promotes Tumorigenesis in a Transgenic Mouse Model of NSCLC

To determine the role of PML inactivation in lung tumorigenesis in vivo, we studied the effects of *Pml* loss in a doxycycline (doxy) inducible compound transgenic mutant model of K-Ras^{G12D}-induced NSCLC (Fisher et al., 1999). We crossed tetracycline operator-regulated K-Ras^{G12D} (Tet-op-K-Ras^{G12D}) responder mice and Clara cell secretory protein-tet activator (CCSP-rtTA) mice into a *Pml* null background (Wang et al., 1998). Lung tumorigenesis was compared after 8 weeks of doxy treatment. *Pml* mice had a significantly increased tumor burden as compared to wild-type animals (Figure 7A). Furthermore, *Pml*$^{-/-}$ tumors displayed several features consistent with a more malignant phenotype. Tumors arising in a wild-type background have a round architecture and mildly atypical nuclei. By contrast, *Pml*$^{-/-}$ tumors have irregular borders and display a higher histologic grade, with cells markedly pleomorphic with increased nuclear/cytoplasmic ratios and atypical nuclei. In addition, *Pml*$^{-/-}$ mutants display increased mitotic activity and a marked decrease in the induction of the cellular senescence markers p21 and p16, which are known to be upregulated in murine lung models of Ras-induced tumorigenesis (Figure 7B) (Collado et al., 2005). These results provide strong genetic evidence that loss of PML tumor-suppressive function in the lung plays an important role in NSCLC tumorigenesis, suggesting in turn that pharmacologic restoration of PML expression may be of therapeutic value.

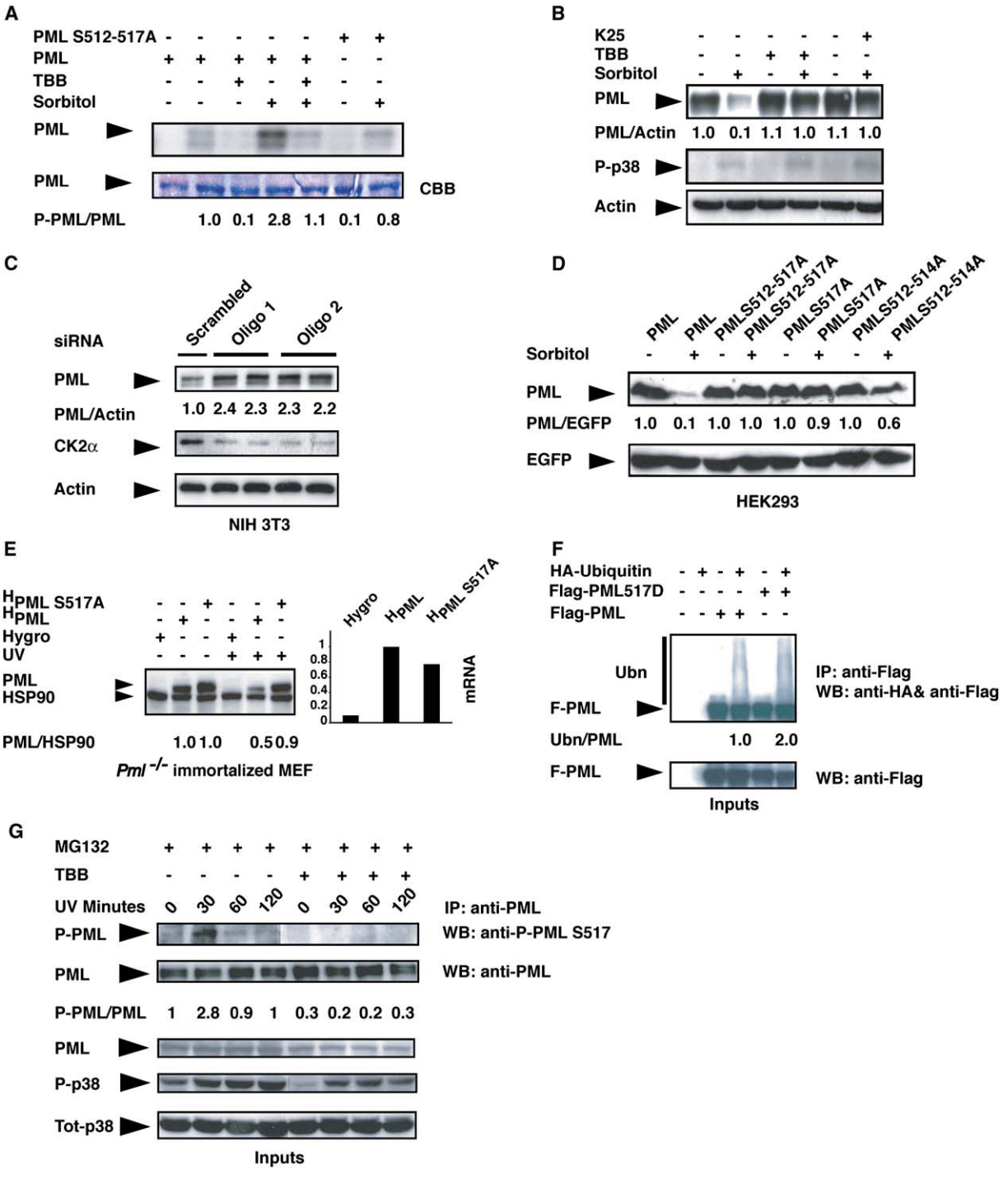

Figure 4. CK2 Is Required for PML Polyubiquitylation

(A) CK2 is activated by osmotic shock, and its activity is required for PML phosphorylation. HEK293 cells were treated with sorbitol as indicated, and their lysates were incubated with bacterially produced His-PML and His-PML S517A. Treatment with TBB was started 1 hr prior to sorbitol and continued for the duration of the experiment. Nickel-bead-immobilized PML proteins were incubated in a kinase assay with γ-ATP, resolved by SDS-PAGE, and autoradiographed. CBB = Coomassie brilliant blue.

(B) Sorbitol-induced PML degradation is dependent on CK2. HEK293 cells were treated as indicated with sorbitol, TBB, or K25, and their lysates were analyzed by WB.

(C) CK2 silencing results in PML protein upregulation. NIH 3T3 cells were transfected with CK2-specific (Oligo 1 and Oligo 2) or scrambled siRNA oligonucleotides. PML, CK2α, and actin proteins were detected by WB.

PML Protein Levels and CK2 Kinase Activity Inversely Correlate in Primary Human NSCLC

We evaluated PML protein levels by WB in 18 primary NSCLC specimens and their unaffected counterpart tissues that were snap frozen at the time of their surgical resection. We found that PML protein was reduced by at least 50% in 10 out of the 18 tumors analyzed, as compared to the unaffected tissue. CK2 kinase activity was increased by at least 50% in 10 tumors (Figure 7C). Importantly, we found a strong association between elevated CK2 kinase activity and decreased PML protein level ($p = 0.002$; Figure 7C). Furthermore, we also found a strong statistical correlation between activation of p38 MAPK and decreased PML protein levels (Figure S6). These observations strongly suggest that elevated CK2 kinase activity leads to PML degradation in primary human NSCLC.

In Vivo CK2 Tumor Inhibition Is Differentially Sensitive to Wild-Type or PML S517A Status

We tested whether CK2 pharmacologic inhibition led to significant antitumor effects and whether wild-type PML and PML S517A lend a differential sensitivity to this treatment in vivo. For these experiments, we used emodin, a specific CK2 inhibitor (Yamada et al., 2005). As expected, emodin upregulated PML, but not PML S517A, in cultured Colo320DM cells. Treatment with emodin in vivo exerted a striking antitumor effect in Colo320DM cells expressing PML, while it was inactive in Colo320DM cells expressing PML S517A (Figure 7D). These results suggest that the inhibition of tumor growth in this experimental setting is in great part due to increased PML protein levels, adding further support to our conclusion that Ser517 is a critical determinant of PML degradation upon CK2 phosphorylation.

DISCUSSION

PML has been the subject of intense investigation due to its multiple tumor-suppressive functions and its ability to regulate key tumor-suppressive pathways. PML protein levels are upregulated at the transcriptional level by p53 and interferon (de Stanchina et al., 2004; Lavau et al., 1995). However, very little is known regarding the mechanisms that control PML protein levels posttranscriptionally, which is of critical relevance since PML is frequently lost through a posttranslational mechanism in prevalent human malignancies (Gurrieri et al., 2004; Koken et al., 1995). Our findings define the first pathway that negatively regulates PML levels in both oncogenic and physiological conditions and establish that pharmacologic CK2 inhibition restores PML function, counteracting tumorigenicity in vivo.

In mammalian cells, p38 MAPK is strongly activated in response to stress stimuli ranging from osmotic shock to UV and ionizing radiation to inflammatory cytokines, resulting in CK2 activation (Kato et al., 2003; Roux and Blenis, 2004). This pathway plays an essential role in regulating inflammation, cell differentiation, cell growth, and apoptosis. Despite the fact that p38 MAPK activation is generally regarded as proapoptotic, there is evidence that p38 MAPK activation can also protect from apoptosis depending on cellular context and stimulus and can play a causal role in human tumorigenesis (Elenitoba-Johnson et al., 2003; Esteva et al., 2004; Kato et al., 2003).

Traditionally, CK2 has been regarded as a constitutively active, ubiquitous serine/threonine protein kinase in search of specific physiological functions (Pinna, 2002). However, several studies have indicated that CK2 plays a critical role in the regulation of cell proliferation and survival (Ahmed et al., 2002). The molecular pathways modulating the prosurvival properties of CK2 have remained largely unknown, with the exception of its role in cellular UV response. In this setting, CK2 is activated by UV radiation in a p38 MAPK-dependent manner, leading to phosphorylation and degradation of the NF-κB inhibitor IκBα (Kato et al., 2003). Furthermore, upon UV irradiation, CK2 complexes and phosphorylates p53 at Ser389. MEF cells and mice carrying the p53 S389A mutant in the p53 locus have defects in the induction of p53 target genes and apoptosis and exhibit increased skin tumorigenesis upon UV irradiation (Bruins et al., 2004; Keller et al., 2001). Conversely, wild-type p53 inhibits CK2 protein kinase (Schuster et al., 2001). These observations support the notion that p53 and CK2 functions are interconnected in a tightly regulated network.

Our work defines a functional network between p38 MAPK, p53, CK2, and PML (Figure 7E). In addition to its well-established role as a p53 coactivator during genotoxic stress (Bernardi et al., 2004; Guo et al., 2000; Salomoni and Pandolfi, 2002), PML regulates UV response by inducing apoptosis or cell-cycle arrest in a p53-independent manner (Salomoni et al., 2005). In this context, the phosphorylation of PML by CK2 (and the concomitant phosphorylation of IκBα by CK2) is part of

(D) PML mutants carrying mutations that impair CK2 phosphorylation are resistant to sorbitol-induced degradation. HEK293 cells were transfected with wild-type and PML degron mutant plasmids and treated for 1 hr with sorbitol as indicated. PML and EGFP protein levels were detected by WB.
(E) A PML mutant carrying a mutation that abrogates the primary CK2 phosphorylation site is resistant to UV-induced degradation. *Pml*$^{-/-}$ immortalized MEF cells were transduced with the indicated retroviral vectors, and, after drug selection, their lysates were analyzed by WB. The PML/heat shock protein 90 (HSP90) ratio is provided. Histogram: real-time RT-PCR quantification of the indicated mRNA in transduced cells.
(F) A phosphomimetic PML S517D mutant displays increased polyubiquitylation. HEK293 cells were transfected as indicated, and their cell lysates were analyzed as indicated. Ten percent of the input lysate was analyzed by WB (lower panel).
(G) PML is phosphorylated upon UV treatment. NIH 3T3 cells were treated with UV radiation, MG132, and TBB as indicated. Treatment with MG132 and TBB was started 1 hr prior to UV radiation. Endogenous P-PML S517 was detected after IP and WB with the indicated antibodies. The membrane was stripped in between hybridizations. Lower panels: Ten percent of the IP input was analyzed by WB.

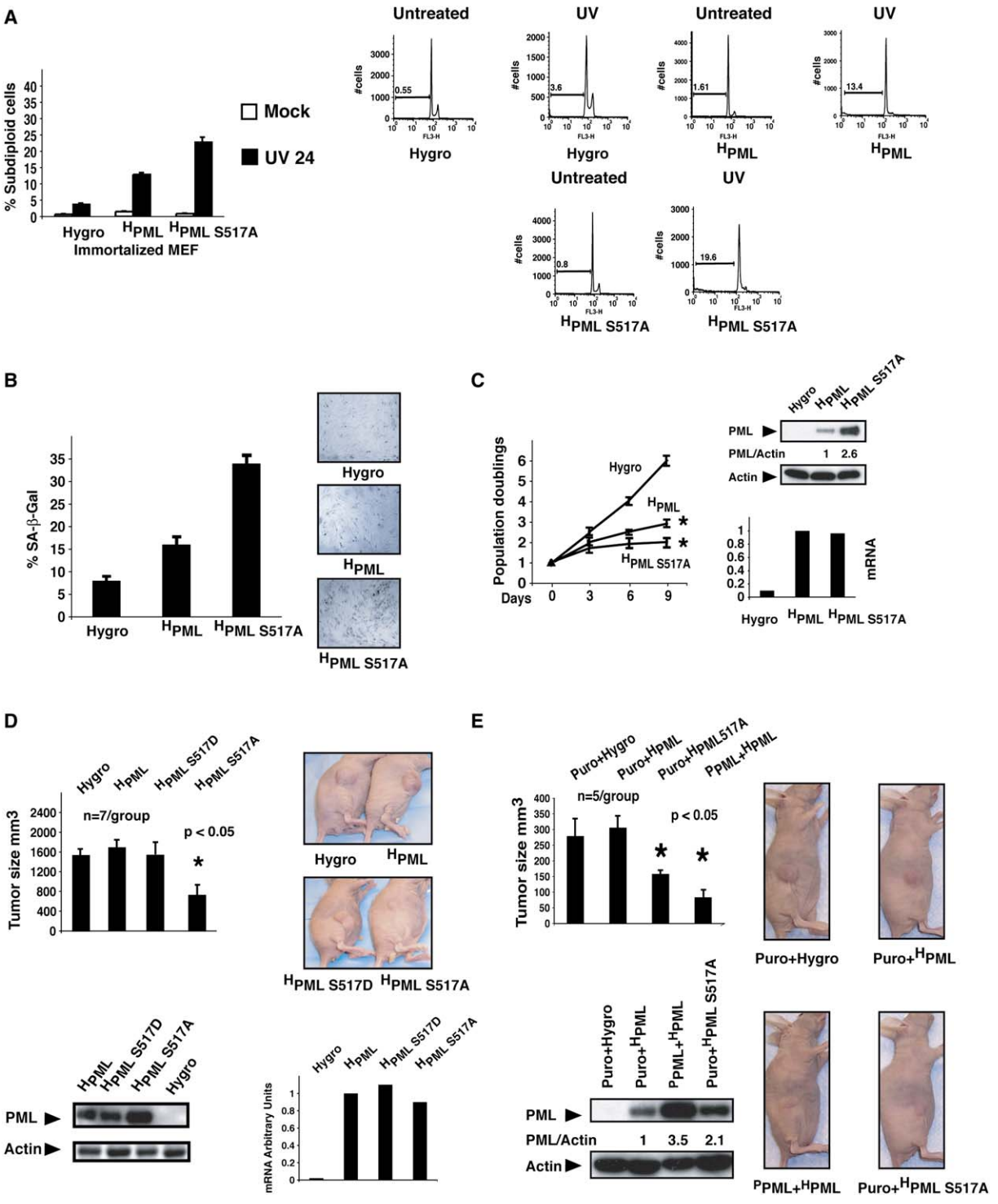

Figure 5. Mutation of the CK2 Phosphorylation Site Alters PML Tumor-Suppressive Properties

(A) PML S517A induces increased apoptosis upon UV treatment. The histogram shows the percentage of apoptosis in retrovirally transduced immortalized *Pml*$^{-/-}$ MEF measured in untreated cells and 24 hr after UV radiation. Apoptosis was measured by subdiploid-peak analysis. Representative cell-cycle profiles are shown on the right. All error bars represent standard deviation.

(B) PML S517A induces increased senescence in WI38 cells. Cells were transduced with the indicated retroviral vectors. The histogram shows the percentage of SA-β-Gal staining 6 days after completion of drug selection. Three hundred cells were scored in a representative field per plate. The results are the mean value of triplicates. Contrast phase photographs of a representative experiment are shown on the right.

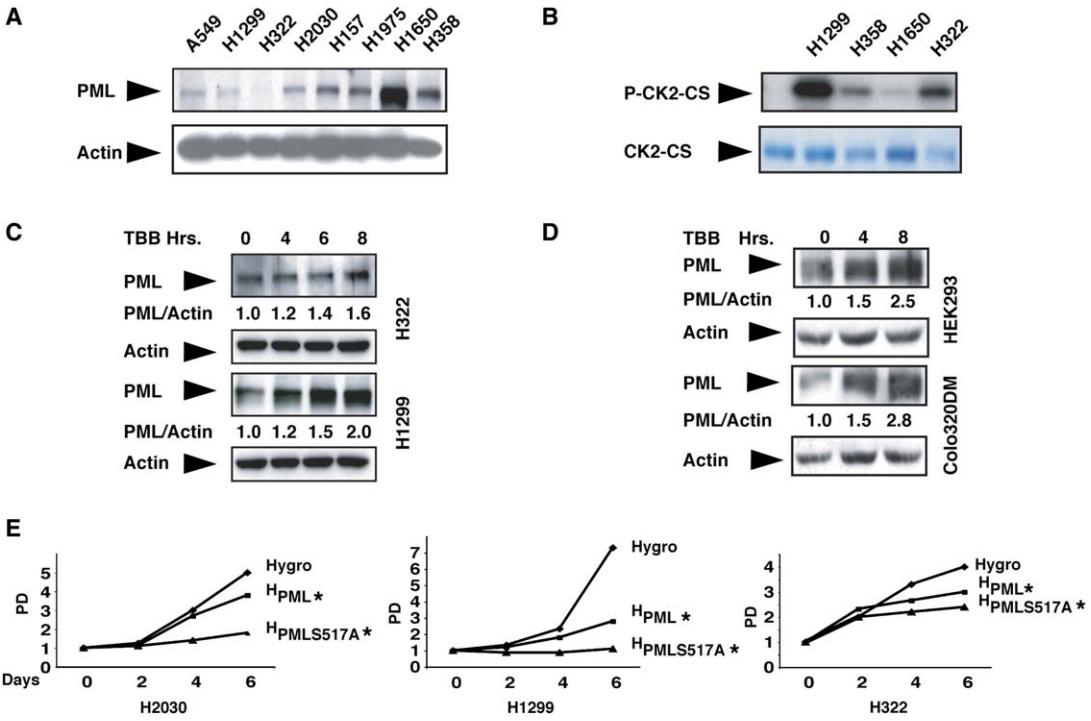

Figure 6. Elevated CK2 Kinase Activity Leads to PML Degradation in Tumor Cell Lines

(A) PML protein levels and CK2 kinase activity are inversely correlated in NSCLC cell lines. PML and actin proteins were detected by WB in the indicated NSCLC cell lines.

(B) CK2 kinase activity and PML protein are inversely correlated in NSCLC cell lines. Upper panel: CK2-CS, a recombinant CK2 substrate, was incubated with lysates of the indicated cell lines. CK2-CS was bound to GST beads, incubated in a kinase assay with γ-ATP, resolved by SDS-PAGE, and autoradiographed. P-CK2-CS: phosphorylated CK2-CS. Coomassie blue staining of input CK2-CS is shown (lower panel).

(C) Pharmacologic inhibition of CK2 restores PML protein levels in H1299 and H322 cells. Cell lines were incubated with TBB and analyzed by WB as indicated.

(D) Pharmacologic inhibition of CK2 restores PML protein levels in HEK293 and Colo320DM cells. Cell lines were incubated with TBB and indicated and analyzed by WB.

(E) PML S517A has increased growth-suppressive abilities in NSCLC-derived cells. Growth curves of H2030, H1299, and H322 cells transduced as indicated are shown. The cells were fixed on the indicated days and stained with crystal violet. Day 0 is the first day after completion of drug selection. * = statistically significant difference between the indicated cells and cells transduced with empty Hygro vector. Please note that standard deviations were too small to appear in the scale of this graph. PD = population doublings.

a cellular circuitry that attenuates apoptosis, allowing cells to recover from noxious stimuli.

Under conditions of oncogenic stress, such as the ones triggered by oncogenic Ras, PML is activated and exerts its tumor-suppressive function in concert with several partners, including p53. In this context, p53 may inhibit CK2 to achieve maximal PML activity and tumor-suppressive effects. On the contrary, when CK2 kinase activity is upregulated (as often happens in human cancers), PML is polyubiquitylated and degraded (Figure 7E). This

(C) PML S517A induces increased growth suppression in WI38 cells. The histogram shows the growth curve of WI38 cells expressing the indicated proteins. Population doublings for each time point are the mean value of triplicates. Day 0 is the first day after completion of drug selection. Upper right: WB showing transduced proteins. Lower right: real-time RT-PCR quantification of the indicated mRNA in transduced cells.

(D) In vivo tumorigenesis of Colo320DM cells expressing wild-type or mutant PML proteins. Cells were transduced with the indicated retroviral vectors and injected subcutaneously in nude mice. Left panel: histogram showing a representative experiment along with standard deviations (7 mice/group). The size of the tumors was analyzed by Student's t test 4 weeks after injection. * = statistically significant differences between the tumors expressing PML and PML S517A. Right panels: representative examples of injected mice. Lower left panels: WB of an aliquot of the Colo320DM cell lines after drug selection. Lower right panel: real-time RT-PCR quantification of the indicated mRNA in transduced cells.

(E) PML overexpression is growth suppressive in vivo. Cells were cotransduced with the indicated retroviral vectors and injected subcutaneously in nude mice. Left panel: histogram showing a representative experiment along with standard deviations (5 mice/group). The size of the tumors was analyzed by Student's t test 12 days after tumor cell injection. * = statistically significant differences between the tumors cotransduced with Puro and ^{H}PML S517A or ^{P}PML and ^{H}PML when compared to tumor cotransduced with Puro and Hygro. Right panels: representative examples of injected mice. Lower left panels: WB of an aliquot of the transduced cells before injection.

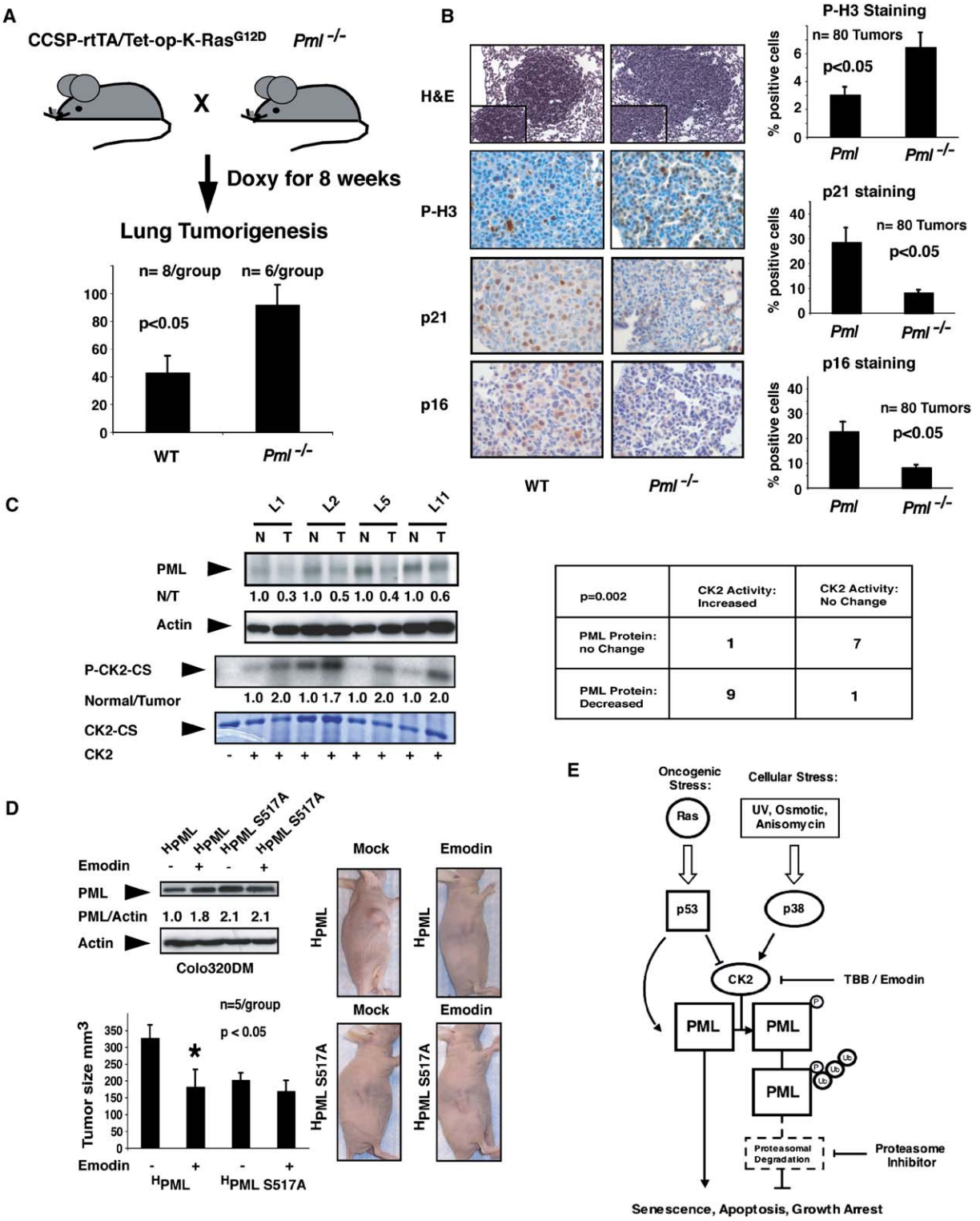

Figure 7. In Vivo Significance of PML Loss in Tumorigenesis

(A) *Pml* inactivation promotes tumorigenesis in a transgenic mouse model of NSCLC. Tet-op-K-Ras^{G12D}/CCSP-rtTA mice were crossed into a *Pml*$^{-/-}$ background. Histogram: quantification of number of adenocardinomas present in each mouse after 8 weeks of doxy treatment. Three representative H&E-stained sections were counted per mouse analyzed. All error bars represent standard deviation.

scenario may be particularly relevant for the pathogenesis of NSCLC, in which increased CK2 kinase activity may occur because of either p38 MAPK activation or *CK2α* gene amplification, a marker of poor prognosis in this disease (O-charoenrat et al., 2004).

The observation that *Pml* loss cooperates with oncogenic Ras in a transgenic mouse model of NSCLC provides further support for our model. In this cascade, by triggering PML degradation, CK2 disables the cellular senescence response to oncogenic Ras. It is noteworthy that Ras and CK2 operate in parallel pathways, as we have found no evidence that oncogenic Ras activates CK2 in MEFs or mouse lung tissue (P.P.S., T.M.Y. and P.P.P., unpublished data). This is also underscored by the fact that CK2 activity and Ras mutations were independent variables in the eight NSCLC cell lines that we utilized (Table S1). PML loss may be further exacerbated in tumors that have also lost p53 function since PML is under the transcriptional control of p53 (de Stanchina et al., 2004).

We therefore propose that therapy with specific CK2 inhibitors or proteasome inhibitors such as bortezomib, which is currently used in the treatment of several human cancers (Richardson et al., 2003), may be particularly effective in tumors that display aberrant CK2 activity and loss of PML protein.

EXPERIMENTAL PROCEDURES

Plasmids, Cell Culture, Transfections, and Transactivation Assays

pTAG2 PML expresses Flag-tagged PML IV. The construction of its derivatives and the complete list of plasmids are available in the Supplemental Data. Tumor cell lines were from the ATCC. Amphotropic Phoenix cells were a gift from G. Nolan (Stanford University). Primary and immortalized MEFs were as described (Bernardi et al., 2004). Transfections were performed with Effectene Transfection Reagent (QIAGEN). Luciferase assays were performed 24 hr after transfection by the Dual-Luciferase Reporter Assay System (Promega).

Recombinant Retroviruses

Recombinant retroviruses were generated by transient transfection of Phoenix packaging cell lines. Experimental details are provided in the Supplemental Data.

Immunoblotting, Immunoprecipitations, and Chemicals

Immunoprecipitations (IP) and Western blots (WB) were performed according to standard procedures in RIPA buffer. Membranes were stripped in between hybridizations unless otherwise indicated. Protein amounts were quantified by densitometry, and the results were expressed as a ratio between the specific band under examination and appropriate internal control. Chemicals were from Calbiochem, Sigma, and Invitrogen. The list of the antibodies and chemicals used is in the Supplemental Data.

RNA Interference and Quantitative Real-Time RT-PCR

NIH 3T3 cells were transfected with CK2α siRNA duplexes (CSNK2A1 siRNA/siAb Assay Kit, Upstate, cat. # 60-013) or nonspecific control SMARTpool siRNA using siRNA DharmaFECT Transfection Reagent (Dharmacon). Cells were analyzed by WB 48 hr after transfection. Quantitative real-time RT-PCR was performed on a Roche LightCycler System using retroviral and hypoxanthine phosphoribosyl transferase or porphobilinogen deaminase-specific primers.

Half-Life Determination

Unmanipulated or transfected cells were exposed to 20 μg/ml cycloheximide and harvested at different time points, and the extracts were analyzed by WB.

In Vivo PML Degradation and Ubiquitylation Assays

HEK293 cells were transiently transfected with plasmids expressing wild-type or mutant PML with HA-tagged ubiquitin (HA-Ub). In most of the experiments, the proteasome inhibitors MG132 and lactacystin (20 μM) or their solvent DMSO (0.2%) was added 6 hr before harvesting. PML-ubiquitin conjugates were analyzed by IP-WB.

Immunofluorescence and Immunohistochemistry Microscopy

These experiments were performed as described (Gurrieri et al., 2004). Details are provided in the Supplemental Data.

Bacterially Produced PML Proteins and In Vitro CK2 Kinase Assay

Bacterially expressed histidine-tagged wild-type PML and mutant PML were purified with Ni-NTA agarose beads (QIAexpressionist, QIAGEN). Kinase assays were performed with recombinant CK2 or 20–50 μg of cellular lysate. Recombinant PML proteins and a GST-fusion peptide containing a CK2 consensus site (GST-CS) were used as substrate (Upstate). Details are provided in the Supplemental Data.

In Vitro Phosphorylation-Site Mapping by Mass Spectrometry

Gel-resolved proteins from in vitro phosphorylation reactions were analyzed by matrix-assisted laser desorption/ionization reflectron time-of-flight (MALDI-reTOF) mass spectrometry (MS) (Ultraflex TOF/TOF;

(B) Histopathological characterization of NSCLC in $Pml^{-/-}$ mice. Lung sections of wild-type and $Pml^{-/-}$ mice were stained as indicated. Representative 400× magnification images are shown. The percentage of positive cells was determined by counting 20 tumors present on representative sections of four mice for each genotype (histograms on the right). For each staining, the difference was statistically significant.

(C) PML protein levels and CK2 kinase activity inversely correlate in primary human NSCLC. PML protein was detected by WB in primary NSCLC specimens and their uninvolved adjacent tissue. Upper panel: analysis of four representative cases. PML protein levels were compared between paired normal (N) and tumor (T) tissues. Lower panels: The same lysates were used to perform a CK2 kinase assay with the CK2-CS substrate. P-CK2-CS was visualized by autoradiography after SDS-PAGE. Coomassie blue staining of input CK2-CS is provided. L1, L2, L5, and L11: individual NSCLC cases. Right panel: Fisher's test analysis of all 18 NSCLCs and their unaffected surrounding tissue.

(D) In vivo CK2 tumor inhibition is differentially sensitive to wild-type or PML S517A status. Left panels: WB analysis of Colo320DM cells expressing PML or PML S517A were treated with emodin (50 μg/ml) as indicated for 4 hr. Notice that PML S517A-expressing cells are insensitive to treatment. The same cells were injected subcutaneously in nude mice. Mice received emodin as indicated. Histogram: representative experiment along with standard deviations (5 mice/group). The size of the tumors was analyzed by Student's t test 12 days after emodin treatment. * = statistically significant difference between untreated and treated cells. Right panels: representative examples of mice after tumor cell injection and treatment.

(E) Molecular mechanisms controlling PML polyubiquitylation. During the cellular response to stress, CK2 kinase controls PML protein levels through integration of upstream p53 and p38 MAPK signals. Therapy with CK2 or proteasome inhibitors will abrogate aberrant PML protein degradation, leading to restoration of PML tumor-suppressive properties.

Bruker) (Winkler et al., 2002). Experimental details are provided in the Supplemental Data.

Generation of Compound Mutant Mice, In Vivo Tumorigenesis, and Emodin Treatment

Pml$^{-/-}$, CCSP-rtTA, and Tet-op-K-Ras^{G12D} transgenic mice were bred to generate compound mutant mice (Fisher et al., 1999; Tichelaar et al., 2000; Wang et al., 1998). Starting at 8 weeks of age, mice were maintained either on standard or doxycycline-impregnated food pellets for 8 weeks (Harlan Teklad). Lungs were collected as described, and tumor burden in individual mice was assessed in three representative hematoxylin-and-eosin-stained sections (Fisher et al., 1999). Xenograft experiments were performed with 10^7 retrovirally transduced cells and were repeated at least twice with identical results. Emodin was administered intraperitoneally 4 days after tumor cell injection and continued daily for 12 days (Yamada et al., 2005). All animal studies were performed in accordance with the guidelines of the MSKCC Institutional Animal Care and Use Committee. Details are provided in the Supplemental Data.

Determination of Apoptosis, Replicative Senescence, and Growth Kinetics

Hypodiploid events, cell growth kinetics, and senescence-associated β-galactosidase (SA-β-Gal) assay were performed according to standard procedures. Details are provided in the Supplemental Data.

Non-Small Cell Lung Cancer Analysis

NSCLC surgical specimens were consecutively collected at Memorial Sloan-Kettering Cancer Center. At the time of surgical resection, a sample of tumor tissue as well as uninvolved adjacent lung was snap frozen. The initial diagnosis was confirmed by hematoxylin and eosin staining of cryosections. Samples that either were free of tumor or contained more than 90% tumor tissue were analyzed. The study was conducted according to the guidelines of the MSKCC Institutional Review Board.

Supplemental Data

Supplemental Data include Supplemental Experimental Procedures, Supplemental References, six figures, and one table and can be found with this article online at http://www.cell.com/cgi/content/full/126/2/269/DC1/.

ACKNOWLEDGMENTS

We thank Drs. Rosa Bernardi, Zhenbang Chen, Takahiro Maeda, Michele Pagano, Lorenzo Pinna, Andrea Alimonti, and Xuejun Jiang for sharing reagents and advice. We are grateful to Drs. Harold E. Varmus and William Pao for providing the CC10-rtTA and Tet-op-K-Ras transgenic mice. We thank Tulio Matos, Vincent Mahi, and Lynne Lacomis for technical assistance and Pauline Bonner for pathology data management. This work was supported by NIH grant R01 CA71692 to P.P.P. and NCI Cancer Center Support Grant P30 CA08748 to P.T. P.P.S. received support from the ASCO YIA, the CALGB Oncology Fellows Award, the Charles A. Dana Foundation, the Michael and Ethel L. Cohen Foundation, the Steps for Breath Foundation, and NIH K08 grant CA112325-01.

Received: December 22, 2005
Revised: March 28, 2006
Accepted: May 15, 2006
Published: July 27, 2006

REFERENCES

Ahmed, K., Gerber, D.A., and Cochet, C. (2002). Joining the cell survival squad: an emerging role for protein kinase CK2. Trends Cell Biol. *12*, 226–230.

Allende, J.E., and Allende, C.C. (1995). Protein kinases. 4. Protein kinase CK2: an enzyme with multiple substrates and a puzzling regulation. FASEB J. *9*, 313–323.

Bernardi, R., Scaglioni, P.P., Bergmann, S., Horn, H.F., Vousden, K.H., and Pandolfi, P.P. (2004). PML regulates p53 stability by sequestering Mdm2 to the nucleolus. Nat. Cell Biol. *6*, 665–672.

Bischof, O., Kirsh, O., Pearson, M., Itahana, K., Pelicci, P.G., and Dejean, A. (2002). Deconstructing PML-induced premature senescence. EMBO J. *21*, 3358–3369.

Bruins, W., Zwart, E., Attardi, L.D., Iwakuma, T., Hoogervorst, E.M., Beems, R.B., Miranda, B., van Oostrom, C.T., van den Berg, J., van den Aardweg, G.J., et al. (2004). Increased sensitivity to UV radiation in mice with a p53 point mutation at Ser389. Mol. Cell. Biol. *24*, 8884–8894.

Collado, M., Gil, J., Efeyan, A., Guerra, C., Schuhmacher, A.J., Barradas, M., Benguria, A., Zaballos, A., Flores, J.M., Barbacid, M., et al. (2005). Tumour biology: senescence in premalignant tumours. Nature *436*, 642.

de Stanchina, E., Querido, E., Narita, M., Davuluri, R.V., Pandolfi, P.P., Ferbeyre, G., and Lowe, S.W. (2004). PML is a direct p53 target that modulates p53 effector functions. Mol. Cell *13*, 523–535.

Elenitoba-Johnson, K.S., Jenson, S.D., Abbott, R.T., Palais, R.A., Bohling, S.D., Lin, Z., Tripp, S., Shami, P.J., Wang, L.Y., Coupland, R.W., et al. (2003). Involvement of multiple signaling pathways in follicular lymphoma transformation: p38-mitogen-activated protein kinase as a target for therapy. Proc. Natl. Acad. Sci. USA *100*, 7259–7264.

Esteva, F.J., Sahin, A.A., Smith, T.L., Yang, Y., Pusztai, L., Nahta, R., Buchholz, T.A., Buzdar, A.U., Hortobagyi, G.N., and Bacus, S.S. (2004). Prognostic significance of phosphorylated P38 mitogen-activated protein kinase and HER-2 expression in lymph node-positive breast carcinoma. Cancer *100*, 499–506.

Everett, R.D. (2001). DNA viruses and viral proteins that interact with PML nuclear bodies. Oncogene *20*, 7266–7273.

Fisher, G.H., Orsulic, S., Holland, E., Hively, W.P., Li, Y., Lewis, B.C., Williams, B.O., and Varmus, H.E. (1999). Development of a flexible and specific gene delivery system for production of murine tumor models. Oncogene *18*, 5253–5260.

Guo, A., Salomoni, P., Luo, J., Shih, A., Zhong, S., Gu, W., and Pandolfi, P.P. (2000). The function of PML in p53-dependent apoptosis. Nat. Cell Biol. *2*, 730–736.

Gurrieri, C., Capodieci, P., Bernardi, R., Scaglioni, P.P., Nafa, K., Rush, L.J., Verbel, D.A., Cordon-Cardo, C., and Pandolfi, P.P. (2004). Loss of the tumor suppressor PML in human cancers of multiple histologic origins. J. Natl. Cancer Inst. *96*, 269–279.

Hayakawa, F., and Privalsky, M.L. (2004). Phosphorylation of PML by mitogen-activated protein kinases plays a key role in arsenic trioxide-mediated apoptosis. Cancer Cell *5*, 389–401.

Kato, T., Jr., Delhase, M., Hoffmann, A., and Karin, M. (2003). CK2 Is a C-Terminal IkappaB Kinase Responsible for NF-kappaB Activation during the UV Response. Mol. Cell *12*, 829–839.

Keller, D.M., Zeng, X., Wang, Y., Zhang, Q.H., Kapoor, M., Shu, H., Goodman, R., Lozano, G., Zhao, Y., and Lu, H. (2001). A DNA damage-induced p53 serine 392 kinase complex contains CK2, hSpt16, and SSRP1. Mol. Cell *7*, 283–292.

Koken, M.H., Linares-Cruz, G., Quignon, F., Viron, A., Chelbi-Alix, M.K., Sobczak-Thepot, J., Juhlin, L., Degos, L., Calvo, F., and de The, H. (1995). The PML growth-suppressor has an altered expression in human oncogenesis. Oncogene *10*, 1315–1324.

Lallemand-Breitenbach, V., Zhu, J., Puvion, F., Koken, M., Honore, N., Doubeikovsky, A., Duprez, E., Pandolfi, P.P., Puvion, E., Freemont, P., and de The, H. (2001). Role of promyelocytic leukemia (PML) sumolation in nuclear body formation, 11S proteasome recruitment, and

As2O3-induced PML or PML/retinoic acid receptor alpha degradation. J. Exp. Med. *193*, 1361–1371.

Landesman-Bollag, E., Romieu-Mourez, R., Song, D.H., Sonenshein, G.E., Cardiff, R.D., and Seldin, D.C. (2001). Protein kinase CK2 in mammary gland tumorigenesis. Oncogene *20*, 3247–3257.

Lavau, C., Marchio, A., Fagioli, M., Jansen, J., Falini, B., Lebon, P., Grosveld, F., Pandolfi, P.P., Pelicci, P.G., and Dejean, A. (1995). The acute promyelocytic leukaemia-associated PML gene is induced by interferon. Oncogene *11*, 871–876.

Litchfield, D.W. (2003). Protein kinase CK2: structure, regulation and role in cellular decisions of life and death. Biochem. J. *369*, 1–15.

Meggio, F., and Pinna, L.A. (2003). One-thousand-and-one substrates of protein kinase CK2? FASEB J. *17*, 349–368.

Meggio, F., Marchiori, F., Borin, G., Chessa, G., and Pinna, L.A. (1984). Synthetic peptides including acidic clusters as substrates and inhibitors of rat liver casein kinase TS (type-2). J. Biol. Chem. *259*, 14576–14579.

Michael, D., and Oren, M. (2002). The p53 and Mdm2 families in cancer. Curr. Opin. Genet. Dev. *12*, 53–59.

O-charoenrat, P., Rusch, V., Talbot, S.G., Sarkaria, I., Viale, A., Socci, N., Ngai, I., Rao, P., and Singh, B. (2004). Casein kinase II alpha subunit and C1-inhibitor are independent predictors of outcome in patients with squamous cell carcinoma of the lung. Clin. Cancer Res. *10*, 5792–5803.

Pagano, M., and Benmaamar, R. (2003). When protein destruction runs amok, malignancy is on the loose. Cancer Cell *4*, 251–256.

Piazza, F., Gurrieri, C., and Pandolfi, P.P. (2001). The theory of APL. Oncogene *20*, 7216–7222.

Pinna, L.A. (2002). Protein kinase CK2: a challenge to canons. J. Cell Sci. *115*, 3873–3878.

Richardson, P.G., Barlogie, B., Berenson, J., Singhal, S., Jagannath, S., Irwin, D., Rajkumar, S.V., Srkalovic, G., Alsina, M., Alexanian, R., et al. (2003). A phase 2 study of bortezomib in relapsed, refractory myeloma. N. Engl. J. Med. *348*, 2609–2617.

Roux, P.P., and Blenis, J. (2004). ERK and p38 MAPK-activated protein kinases: a family of protein kinases with diverse biological functions. Microbiol. Mol. Biol. Rev. *68*, 320–344.

Salomoni, P., and Pandolfi, P.P. (2002). The role of PML in tumor suppression. Cell *108*, 165–170.

Salomoni, P., Bernardi, R., Bergmann, S., Changou, A., Tuttle, S., and Pandolfi, P.P. (2005). The promyelocytic leukemia protein PML regulates c-Jun function in response to DNA damage. Blood *105*, 3686–3690.

Sayed, M., Kim, S.O., Salh, B.S., Issinger, O.G., and Pelech, S.L. (2000). Stress-induced activation of protein kinase CK2 by direct interaction with p38 mitogen-activated protein kinase. J. Biol. Chem. *275*, 16569–16573.

Schuster, N., Gotz, C., Faust, M., Schneider, E., Prowald, A., Jungbluth, A., and Montenarh, M. (2001). Wild-type p53 inhibits protein kinase CK2 activity. J. Cell. Biochem. *81*, 172–183.

Seldin, D.C., and Leder, P. (1995). Casein kinase II alpha transgene-induced murine lymphoma: relation to theileriosis in cattle. Science *267*, 894–897.

Tichelaar, J.W., Lu, W., and Whitsett, J.A. (2000). Conditional expression of fibroblast growth factor-7 in the developing and mature lung. J. Biol. Chem. *275*, 11858–11864.

Trotman, L.C., Alimonti, A., Scaglioni, P.P., Koutcher, J.A., Cordon-Cardo, C., and Pandolfi, P.P. (2006). Identification of a tumour suppressor network opposing nuclear Akt function. Nature *441*, 523–527.

Wang, Z.G., Delva, L., Gaboli, M., Rivi, R., Giorgio, M., Cordon-Cardo, C., Grosveld, F., and Pandolfi, P.P. (1998). Role of PML in cell growth and the retinoic acid pathway. Science *279*, 1547–1551.

Winkler, S.G., Lacomis, L., Philip, J., Erdjument-Bromage, H., Svejstrup, J.Q., and Tempst, P. (2002). Isolation and mass spectrometry of transcription factor complexes. Methods *26*, 260–269.

Wu, W.S., Xu, Z.X., Hittelman, W.N., Salomoni, P., Pandolfi, P.P., and Chang, K.S. (2003). Promyelocytic leukemia protein sensitizes tumor necrosis factor alpha-induced apoptosis by inhibiting the NF-kappaB survival pathway. J. Biol. Chem. *278*, 12294–12304.

Yamada, M., Katsuma, S., Adachi, T., Hirasawa, A., Shiojima, S., Kadowaki, T., Okuno, Y., Koshimizu, T.A., Fujii, S., Sekiya, Y., et al. (2005). Inhibition of protein kinase CK2 prevents the progression of glomerulonephritis. Proc. Natl. Acad. Sci. USA *102*, 7736–7741.

Yang, S., Kuo, C., Bisi, J.E., and Kim, M.K. (2002). PML-dependent apoptosis after DNA damage is regulated by the checkpoint kinase hCds1/Chk2. Nat. Cell Biol. *4*, 865–870.

Zhong, S., Muller, S., Ronchetti, S., Freemont, P.S., Dejean, A., and Pandolfi, P.P. (2000). Role of SUMO-1-modified PML in nuclear body formation. Blood *95*, 2748–2752.